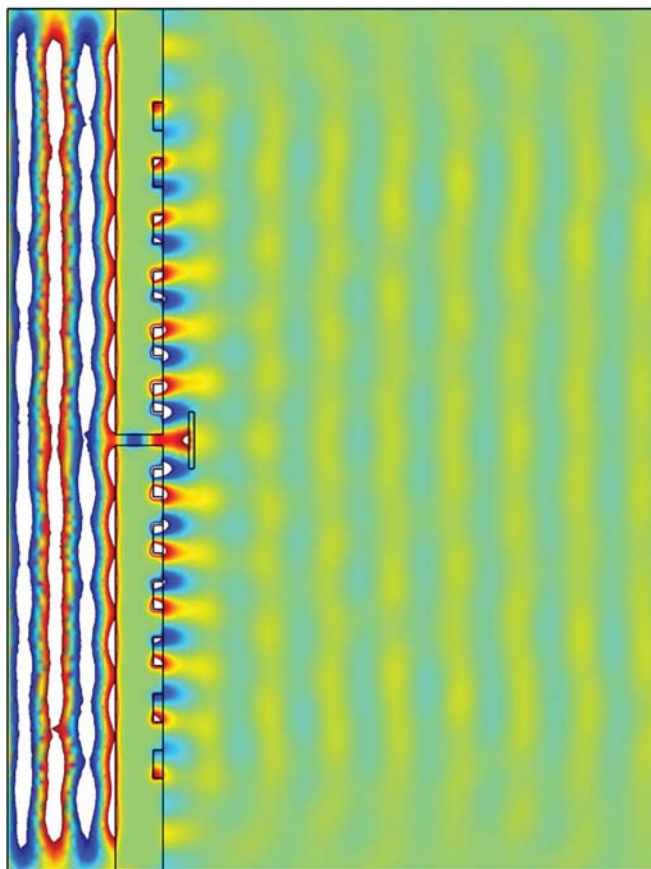


# Near-Field-Resonance-Enhanced Plasmonic Light Beaming

Volume 2, Number 1, February 2010

P. Chen  
Q. Gan  
F. J. Bartoli  
L. Zhu



DOI: 10.1109/JPHOT.2009.2039865  
1943-0655/\$26.00 ©2010 IEEE

# Near-Field-Resonance-Enhanced Plasmonic Light Beaming

Pengyu Chen,<sup>1</sup> Qiaoqiang Gan,<sup>2</sup> Filbert J. Bartoli,<sup>2</sup> and Lin Zhu<sup>1</sup>

<sup>1</sup>Center for Optical Materials Science and Engineering Technologies, Department of Electrical and Computer Engineering, Clemson University, Clemson, SC 29634 USA

<sup>2</sup>Department of Electrical and Computer Engineering, Lehigh University, Bethlehem, PA 18015 USA

DOI: 10.1109/JPHOT.2009.2039865  
1943-0655/\$26.00 © 2010 IEEE

Manuscript received November 23, 2009; revised December 21, 2009. First published Online December 30, 2009. Current version published January 20, 2010. Corresponding author: L. Zhu (e-mail: zhu3@clemson.edu).

**Abstract:** In this paper, we have investigated the enhancement of the plasmonic light beaming efficiency by near-field resonance in different subwavelength metallic slit-groove beaming structures. We show that by selecting the suitable film thickness and separation distance of beaming gratings, the intensity of the near field can be greatly enhanced by resonance, which leads to the increase of the beaming efficiency in the far field. Moreover, we obtain a nanocavity above the nanoslit by integrating a metal nanostrip with a conventional beaming structure. The resonance of this nanocavity can further enhance the near-field intensity and improve the beaming efficiency.

**Index Terms:** Engineered photonics nanostructures, gratings, plasmonics.

## 1. Introduction

It is well known that when light transmits through an isolated subwavelength aperture, such as a hole or a slit in an opaque screen, the transmission is usually very weak and light diffracts in all the directions [1]. However, when light transmits through a metallic subwavelength aperture surrounded with periodic surface corrugations at the output side, it will propagate in a specific direction instead of diffracting into all the directions. This plasmonic beaming phenomenon is discovered by Lezec *et al.* [2] and has attracted a great amount of interest over the years since it can be used to steer light and reduce the beam divergence beyond the diffraction limit in the subwavelength regime. Plasmonic light beaming is mainly due to the interaction between surface plasmons generated from a small aperture and beaming gratings [3]. During the last few years, there are a lot of impressive results in this field: on-axis and off-axis beaming light from subwavelength apertures [4]–[7], light beaming using photonic crystals [8]–[10], and integration of light beaming structures with quantum cascade lasers [11]–[13]. It has also been shown that light beaming through a subwavelength metal slit surrounded by dielectric surface gratings can be very effective [14], [15]. Meanwhile, extraordinary light transmission through subwavelength apertures with periodic surface gratings at the input side has also been extensively studied [16]–[18]. Most recently, by integrating a metal nanostrip with a subwavelength slit at the input side, enhanced light transmission has been observed [19], [20]. Near-field resonance of surface plasmons mainly contributes to these phenomena.

In fact, near-field resonance can also have a great impact on the plasmonic beaming efficiency due to the inherent connection between the near field and far field. When the near-field intensity is enhanced by resonance, more surface plasmon waves will be generated at the metal surface and

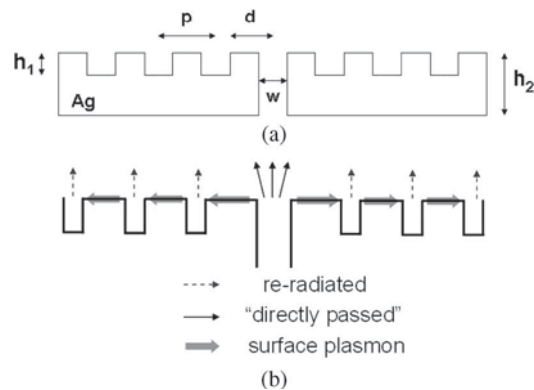


Fig. 1. (a) Symmetric metal gratings on a silver thin film.  $w$  is the slit width,  $p$  is the grating period (center to center),  $h_1$  is the grating depth,  $h_2$  is the film thickness,  $d$  is the grating width, and  $d$  is the separation distance between the first groove and the center of the slit. (b) The dashed arrows are reradiated light, the solid arrows are directly passed light, and the shadow arrows are surface plasmon waves.

subsequently diffracted into the far field by the grating. In this paper, we investigate the plasmonic light beaming effects in the visible region by use of COMSOL Multiphysics. We provide a detailed analysis of the role of near-field resonance in plasmonic light beaming. We first show that a suitable metal film thickness and/or separation distance of beaming gratings of a conventional plasmonic beaming structure [see Fig. 1(a)] can lead to a resonance condition and enhance the near-field intensity, which can increase the beaming efficiency in the far field. We then integrate a metal nanostrip with a conventional beaming structure (see Fig. 7) to form a nanocavity above the metal slit and show that the nanocavity resonance can further enhance the near-field intensity and improve the beaming efficiency.

## 2. Theoretical Analysis

Fig. 1 shows a typical plasmonic beaming structure in a thin silver film. When light transmits through the slit, part of it couples into surface plasmons and propagates along the interface between the metal and air. Some of the illumination light directly travels through the slit and scatters into free space by diffraction. The grating can diffract the energies of surface plasmon waves out of the metal surface and convert them back to light. Thus, the grooves in this beaming structure can be considered as an antenna array.

There are three criteria to evaluate the on-axis beaming efficiency: 1) The far-field light intensity at  $0^\circ$  should be high, which means most of light is diffracted normal to the surface; 2) the full width at half maximum (FWHM) angle of the far-field distribution should be small so that the beamed light has a small divergence; 3) the intensity of the side peaks in the far field should be small. This means that the energy of the diffracted light into other directions is small. According to the Fourier optics theory, in order to satisfy these conditions to obtain a well collimated beam, one of the most important factors is that all the grating grooves in the near field should be in phase. This condition can be satisfied by tuning the grating period  $p$  so that the grating wave vector ( $\mathbf{k}_{G1}$ ) is approximately equal to the surface plasmon wave vector in the grating region ( $\mathbf{k}_{sp-g}$ ). Another important factor is that the near-field intensity should be high. Therefore, if we can obtain the near-field resonance by controlling the geometries of the beaming structure, we can greatly enhance the near-field intensity and the beaming efficiency.

## 3. Simulation Results and Discussions

We use COMSOL to simulate light transmission through the slit-groove beaming structure shown in Fig. 1(a). A plane wave of TM-polarization with the wavelength  $\lambda = 580$  nm is illuminated normally to the input surface. The permittivity of the silver is set to be  $\epsilon_m = -15 + 0.386i$  [21]. The slit width is

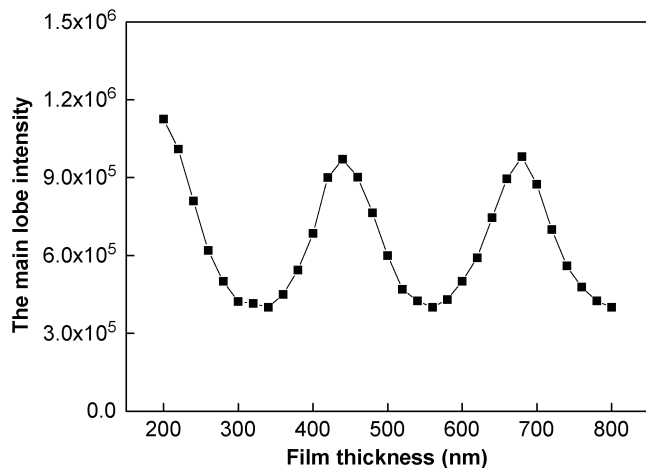


Fig. 2. The main lobe intensity versus the film thickness.

set to be 100 nm in order to get good surface plasmon generation efficiency [22]. The grating depth  $h_1$  is 90 nm and the duty cycle is 50%. We first keep all the parameters the same and only change the grating period to search for the best beaming efficiency. We obtain the optimal beam with a sharp main peak and small side peaks in the far field at  $p = 522$  nm. Therefore, we set  $p = 522$  nm in all simulations. Note that this value is a little bit smaller than the wavelength of surface plasmon at a flat metal surface. This is consistent with previous results [2], [11] and is due to the fact that the surface plasmon wave vector in the grating region ( $\mathbf{k}_{\text{sp-g}}$ ) is different from that in a flat surface ( $\mathbf{k}_{\text{sp-f}}$ ). In the simulation, we also limit the number of the grating period to be six and adopt a perfect matched layer (PML) boundary condition to eliminate unnecessary reflections. Since we are interested in the role of near-field resonance in plasmonic light beaming, we show the electric field intensity in both the near and far fields.

### 3.1. Near-Field Resonance Induced by the Beaming Structure

In this section, we investigate light beaming through a conventional plasmonic beaming structure as shown in Fig. 1(a). We first analyze the Fabry–Pérot-like resonance associated with the nanoslit length (the film thickness)  $h_2$  and its impact on the beaming efficiency. We then show that the second-order Bragg diffraction of the beaming grating can also lead to near-field resonance at the output surface, which is associated with the grating separation distance  $d$ . The simulation results show that by varying the film thickness  $h_2$  and/or the separation distance  $d$ , we can significantly change the near-field intensity, which will further have a great impact on the light beaming efficiency in the far field.

#### 3.1.1. Fabry–Pérot-Like Resonance in the Nanoslit

Although the Fabry–Pérot-like resonance associated with the nanoslit length has been studied in extraordinary optical transmission research [23], [24], we present the results here as they are necessary for a full understanding of the role of the near-field resonance in light beaming.

Here, all the parameters are kept the same as mentioned before and we only change the film thickness from 200 nm to 800 nm. We find that the change of the film thickness does not change the shape of the far field. Fig. 2 shows the far-field main lobe intensity versus the film thickness. The periodic oscillatory behavior manifests the Fabry–Pérot-like resonance in the nanoslit. The near-field intensity at the outside of the slit is enhanced when the constructive interference happens (corresponding to the peak positions in Fig. 2). Therefore, more electromagnetic energy will be diffracted out of the silver surface by the grating, which increases the intensity of the beamed light in the far field.

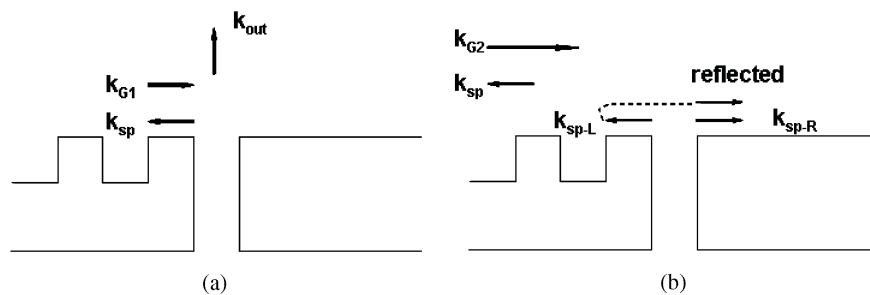


Fig. 3. (a) When  $k_{sp-g}$  is satisfied, the first-order Bragg diffraction ( $m = 1$ ) diffracts the left-going surface plasmons out, normal to the metal surface. (b) The second-order Bragg diffraction ( $m = 2$ ) reflects the left-going surface plasmons into the right-going surface plasmons, which interferes with the original right-going surface plasmons on the thin metal film.

### 3.1.2. Near-Field Resonance Caused by the Second-Order Bragg Diffraction

In addition to the Fabry–Pérot-like resonance in the nanoslit region, the near-field resonance induced by the second-order Bragg diffraction is also of great importance in light beaming. Fig. 4 shows the physics behind this kind of near-field resonance. At the exit surface, when the first-order diffraction wave vector  $k_{G1}$  is equal in magnitude but opposite to the surface plasmon wave vector in the grating region  $k_{sp-g}$ , surface plasmons will be diffracted out normal to the surface due to the conservation of momentum, as shown in Fig. 3(a). Furthermore, due to the second-order Bragg diffraction wave vector  $k_{G2}$ , the left-going surface plasmons will be reflected, propagating toward the right, as shown in Fig. 3(b). Thus there exists the interference between the reflected left-going and original right-going surface plasmons. Depending on the distance  $d$  between the first groove and the center of the slit, these surface plasmon waves can be either in phase or out of phase. This leads to constructive or destructive interference at the metal surface. It should be pointed out that these plasmonic beaming structures are different from the devices reported in [25], where the first-order Bragg diffraction is used to reflect surface plasmons and thus light beaming cannot take place. The total phase difference  $\phi$  between the two interfering surface plasmon waves can be written as a constant phase  $\phi_0$  plus the phase difference associated with their different path lengths along the metal surface:  $\phi = 2k_{sp-r}d + \phi_0$ . The phase constant  $\phi_0$  is determined by the reflection phase and conversion phase between light and surface plasmons as the reflected surface plasmons travel across the slit. Constructive or destructive interference will happen when  $\phi$  equals even or odd multiples of  $\pi$ .

According to our analysis above, we first simulate the light transmission through a single slit in a silver thin film with the grating only on the left side. In order to properly analyze our simulation results, we also defined a parameter, the Surface Enhancement  $E_s$ , which is the electric field energy in the near field with the grating normalized by the one without the grating. We set a line 10 nm away from the top surface of the grating as the near field. Note that the selection of the near field can be very close (less than tens of nanometers) to the surface, and we will obtain the same results:

$$E_s = \int E^2 dl(\text{with grating}) / \int E^2 dl(\text{without grating}). \quad (1)$$

All the parameters are kept the same, and we set the film thickness to be  $h_2 = 440$  nm, where the constructive interference happens in the nanoslit region. Then we change the separation distance  $d$  from 200 nm to 1600 nm with a step of 20 nm. In the simulation, the change of the separation  $d$  dramatically changes the field intensity in the near field. Fig. 4(a) and (b) show the electric field intensity at  $d = 260$  nm and 400 nm. It is clear that at  $d = 260$  nm, we obtain a much stronger field intensity in the near field than that at  $d = 400$  nm at the right side of the metal film surface. We

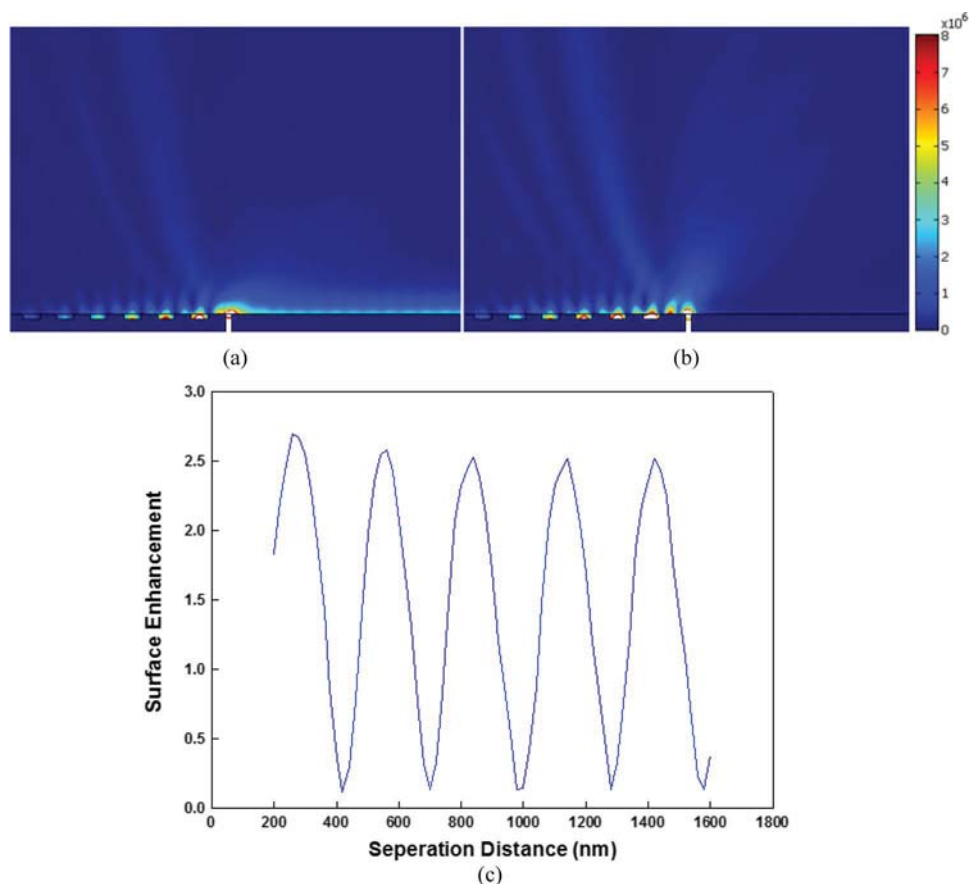


Fig. 4. (a) The electric field intensity in the near field at the separation distance  $d = 260$  nm. (b) The electric field intensity in the near field at the separation distance  $d = 400$  nm. (c) The surface enhancement on the right side of the silver thin film as a function of the separation distance  $d$ .

calculate the surface enhancement of the right side of the film with different separation distances, as shown in Fig. 4(c). In Fig. 4(c), we find that the surface enhancement of the right side of the thin film exhibits an oscillatory behavior as a function of the separation distance  $d$ . This result proves that due to the second-order Bragg diffraction the near-field intensity can be either enhanced or reduced depending on the slit-grating separation distance  $d$ . The initial amplitude fall-off is similar to the optical response of a slit-groove structure reported in [26] and is mainly due to the residual quasicylindrical waves.

In order to understand the relation between the near-field resonance and light beaming, we change the half grating to the symmetric gratings. All the parameters are the same except for the addition of another grating on the right side of the silver film. Fig. 5 shows the simulation results. We show the electric field intensity in the near field and the intensity of the light in the far field for  $d = 260$  nm and 400 nm. In the near field, similar trends have been observed as the half grating structure. The electric field intensity in the near field at  $d = 260$  nm is much greater than that at  $d = 400$  nm. In the far field, a sharp main peak is observed at  $0^\circ$ . This means that most of light propagates normal to the exit surface and efficient light beaming is obtained. While at  $d = 400$  nm, the far field does not show a good beaming efficiency. By comparing Fig. 5(a) and (b), we find that the main lobe intensity of the far field at  $d = 260$  nm is about 30 times larger than that at  $d = 400$  nm.

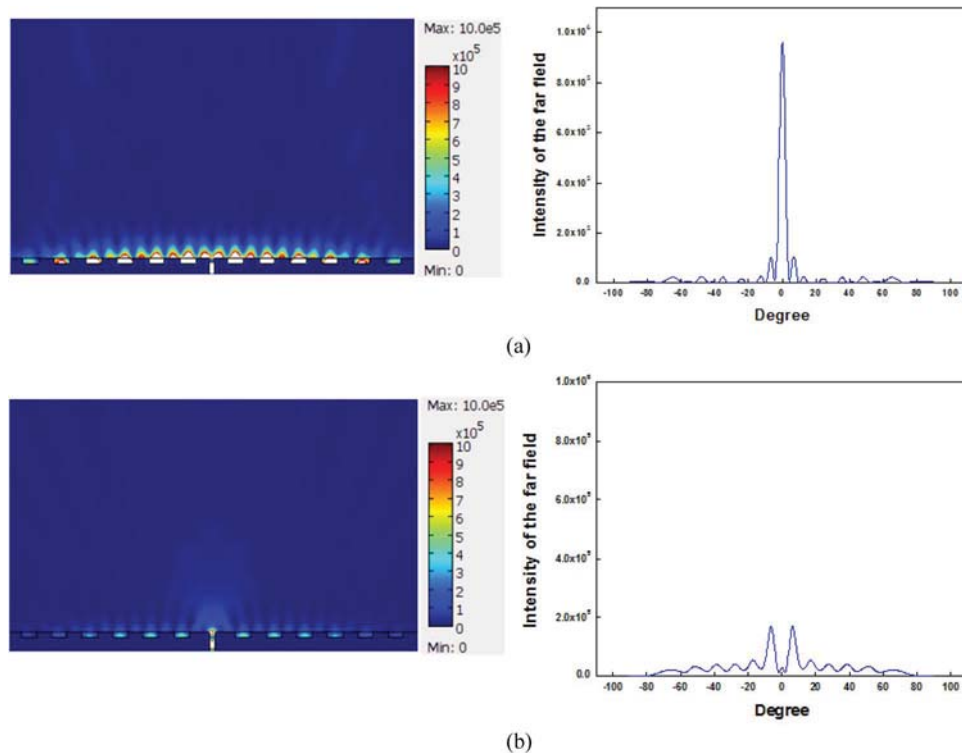


Fig. 5. (a) The electric field intensity in the near field and the intensity of the far field at  $d = 260$  nm. (b) The electric field intensity in the near field and the intensity of the far field at  $d = 400$  nm.

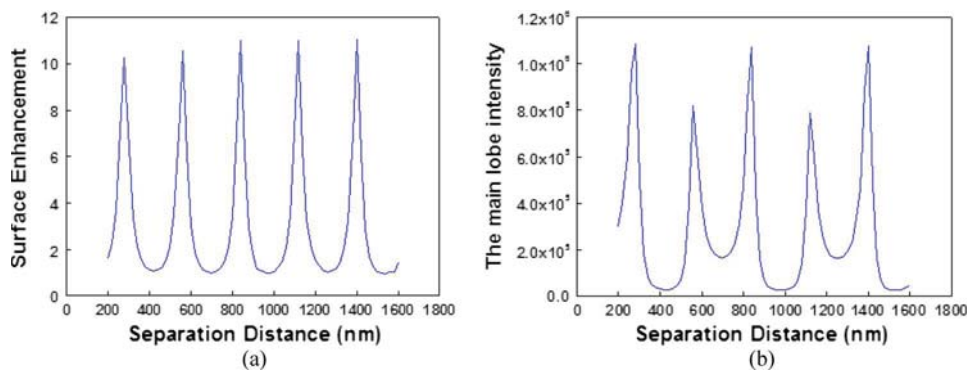


Fig. 6. (a) Surface enhancement of symmetric beaming structures as  $d$  changes from 200 nm to 1600 nm. (b) Main lobe intensity in the far field as  $d$  changes from 200 nm to 1600 nm.

We also obtain the surface enhancement and the main lobe intensity versus the separation distance, as shown in Fig. 6. In Fig. 6, we can find that both the surface enhancement and the main lobe intensity exhibit an oscillatory behavior as a function of the separation distance  $d$ . Their peak values and dip values appear at almost the same positions as in Fig. 4(c), which further confirms our previous analysis. In Fig. 6(b), we can find that the peak values of the main lobe intensity at  $d = 560$  nm and 1120 nm are a little bit smaller than the peak values at  $d = 280$  nm, 840 nm, and 1400 nm. This is mainly due to the interference between the reradiated and “directly passed” light in the far field, as shown in Fig. 1. Since the phase difference between the reradiated and “directly passed” light depends on  $k_{sp-f}d$  (not  $2k_{sp-f}d$ ), we only obtain the maximum beaming efficiency for  $d = 280$  nm, 840 nm, and 1400 nm.

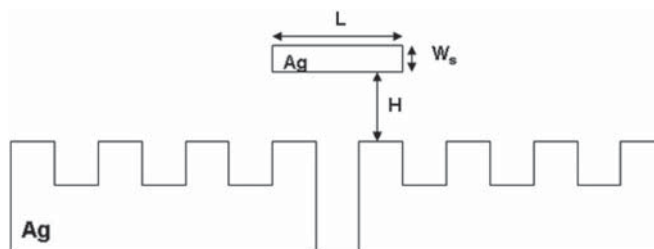


Fig. 7. A composite plasmonic beaming structure integrated with a nanostrip.  $H$  is the distance between the nanostrip and the output surface of the silver thin film.  $W_s$  is the thickness of the nanostrip.  $L$  is the length of the nanostrip.

### 3.2. Near-Field Resonance Induced by an Additional Silver Nanostrip

From the previous discussion, it is clear that the near-field resonance indeed can improve the light beaming efficiency. In this section, we design a nanocavity above the nanoslit by integrating a silver nanostrip with a conventional beaming structure and engineer the nanocavity resonance to further improve the beaming efficiency, as shown in Fig. 7.

When a silver nanostrip is placed on top of the slit at the exit side, a nanocavity can be obtained in the region between the nanostrip and the silver film. By varying the distance  $H$  and nanostrip length  $L$ , the near-field intensity can be either greatly enhanced or reduced depending on the cavity resonance. When the cavity is exactly on resonance, almost all the electromagnetic energy will be confined inside the cavity [19], and very little light can be diffracted into the far field. This is similar to the critical coupling situation within a ring resonator. However, when the cavity is slightly off resonance, the electromagnetic energy inside cavity is still enhanced, and it can couple into surface plasmons in the grating region from two sides. Thus, the near-field intensity and the beaming efficiency will be enhanced. When the cavity is fully off resonance, it should not change the beaming efficiency much. We use COMSOL to simulate light transmission through the composite beaming structure in Fig. 7 and compare the results with the conventional beaming structure in Fig. 1(a). All the grating parameters are set to be the same as Fig. 5(a). The nanostrip is 50 nm thick.

We should consider a few factors when selecting geometrical parameters of this nanocavity. First, in order not to block the reradiated light from the first groove of the grating, the length of the nanostrip  $L$  should be smaller than 520 nm. Second, the distance  $H$  should be smaller than the simulation wavelength of 580 nm to obtain strong impact of the nanocavity on the near-field distribution. We then systematically vary both  $L$  and  $H$  in 10-nm steps to search for the best beaming efficiency. We obtain it for  $L = 520$  nm and  $H = 240$  nm. We show the simulation results and compare with a conventional beaming structure in Fig. 8. From the intensity of the electric field in the near field, it can be clearly found that we can further enhance the near-field intensity by use of the composite beaming structure. In the far field, we find that the main lobe intensity in Fig. 8(b) is around three times bigger than that in Fig. 8(a). This means that more light is diffracted out normal to the output surface. Therefore, the nanocavity resonance can further improve the beaming efficiency.

In order to understand the impact of the cavity resonance induced by the nanocavity in light beaming, we plot out the main lobe intensity in the far field versus the distance  $H$  and the nanostrip length  $L$ . In Fig. 9(a), we find that the main lobe intensity initially falls off and then starts to increase as  $H$  increases. The main lobe intensity achieves its maximum value at  $H = 240$  nm. However, when the distance  $H$  further increases to 260 nm, the main lobe intensity becomes very small. In this situation, most of light is confined in the region between the nanostrip and the film and the near-field intensity outside the nanocavity is very low. This actually corresponds to the exact on-resonance condition of the nanocavity. There are not many surface plasmon waves propagating along the surface. Therefore, the main lobe intensity in the far field is very small and poor beaming is observed. When  $H$  goes beyond half of the wavelength of the illumination light, the influence of the cavity to the intensity of the near field becomes smaller, and the main lobe intensity in the far

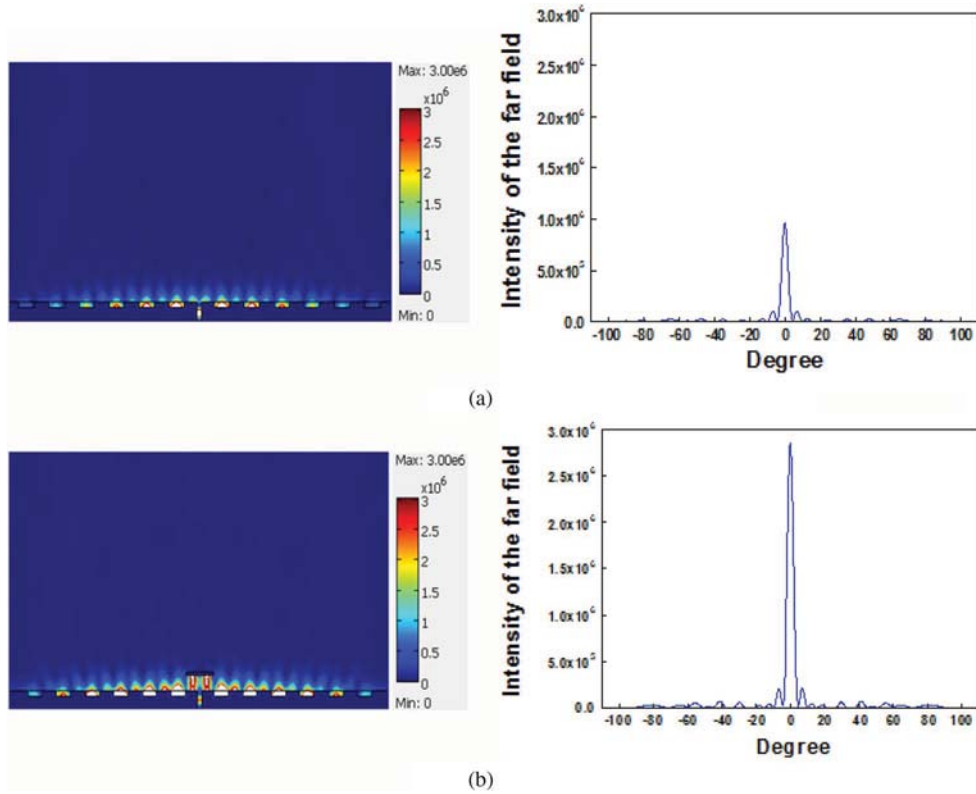


Fig. 8. (a) The electric field intensity in the near field and the intensity of the far field in the conventional beaming structure. (b) The electric field intensity in the near field and the intensity of the far field in the composite beaming structure.

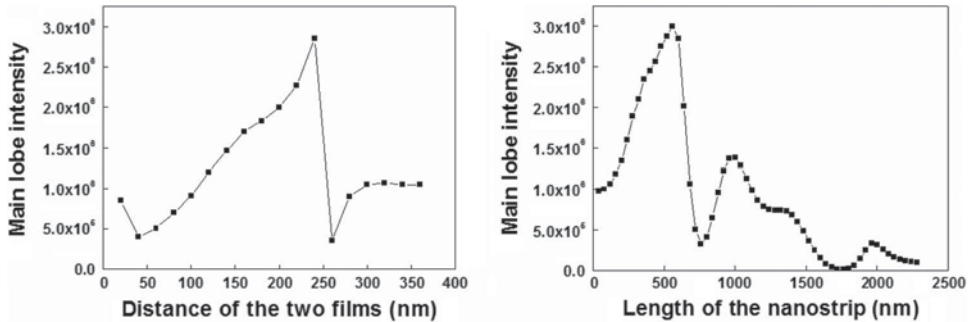


Fig. 9. (a) The main lobe intensity in the far field versus the distance  $H$  between the nanoribbon and the silver thin film. The nanoribbon length is 520 nm. (b) The main lobe intensity in the far field versus the length of the nanoribbon  $L$ . The distance between the nanoribbon and the silver thin film is 240 nm.

field stays almost the same. Fig. 9(b) shows the main lobe intensity in the far field versus the length of the nanoribbon. The oscillatory behavior of the main lobe intensity indicates that the cavity resonance plays an importance role. Again, it shows that the cavity should be slightly off the exact resonance condition to obtain the optimal beaming efficiency. In addition, when  $L$  becomes larger than the separation distance  $d$ , some of the reradiated light will be blocked by the nanoribbon. Thus, the main lobe intensity will be smaller and more side peaks can be observed in the far field.

This composite beaming structure has potential applications as an active plasmonic emitter. By placing gain materials inside the nanocavity of the composite beaming structure, we can not only enhance the emission through the resonance enhancement but also collimate the emitted light through the beam grating.

#### 4. Conclusion

In conclusion, we have studied the role of the near-field resonance in light beaming for different metallic slit-groove beaming structures. We first investigate a conventional metallic slit-groove beaming structure. The simulation results show that the intensity of the beamed light in the far field can be greatly enhanced by the near-field resonance, which is determined by the geometry of the beaming structure. Further optimization of the beaming efficiency can be obtained by integrating a metal nanostrip with a conventional beaming structure. In this composite beaming structure, we can engineer the nanocavity resonance to improve the beaming efficiency. We show that the cavity should be slightly off the exact resonance condition to obtain the optimal beaming efficiency. Controlling collimated light in plasmonic structures is of great importance and can provide wide range applications in various integrated optical devices.

---

#### References

- [1] H. A. Bethe, "Theory of diffraction by small holes," *Phys. Rev.*, vol. 66, no. 7/8, pp. 163–182, Oct. 1944.
- [2] H. J. Lezec, A. Degiron, E. Devaux, R. A. Linke, L. Martin-Moreno, F. J. Garcia-Vidal, and T. W. Ebbesen, "Beaming light from a subwavelength aperture," *Science*, vol. 297, no. 5582, pp. 820–822, Aug. 2002.
- [3] L. B. Yu, D. Z. Lin, Y. C. Chen, Y. C. Chang, K. T. Huang, J. W. Liaw, J. T. Yeh, J. M. Liu, C. S. Yeh, and C. K. Lee, "Physical origin of directional beaming emitted from a subwavelength slit," *Phys. Rev. B, Condens. Matter*, vol. 71, no. 4, p. 041405, Jan. 2005.
- [4] B. Wang and G. P. Wang, "Directional beaming of light from a nanoslit surrounded by metallic heterostructures," *Appl. Phys. Lett.*, vol. 88, no. 1, p. 013114, Jan. 2006.
- [5] J. Zhang and G. P. Wang, "Simultaneous realization of transmission enhancement and directional beaming of dual-wavelength light by a metal nanoslit," *Opt. Express*, vol. 17, no. 12, pp. 9543–9548, Jun. 2009.
- [6] H. Caglayan, I. Bulu, and E. Ozbay, "Off-axis beaming from subwavelength apertures," *J. Appl. Phys.*, vol. 104, no. 7, p. 073108, Oct. 2008.
- [7] X. Zhang and C. F. Li, "Polarization-independent directional beaming of light by a subwavelength metal slit," *Chin. Phys. Lett.*, vol. 26, no. 11, p. 114204, Nov. 2009.
- [8] S. K. Morrison and Y. S. Kivshar, "Engineering of directional emission from photonic-crystal waveguides," *Appl. Phys. Lett.*, vol. 86, no. 8, p. 081110, Feb. 2005.
- [9] W. R. Frei, D. A. Tortorelli, and H. T. Johnson, "Topology optimization of a photonic crystal waveguide termination to maximize directional emission," *Appl. Phys. Lett.*, vol. 86, no. 11, p. 111114, Mar. 2005.
- [10] I. Bulu, H. Caglayan, and E. Ozbay, "Beaming of light and enhanced transmission via surface modes of photonic crystals," *Opt. Lett.*, vol. 30, no. 22, pp. 3078–3080, Nov. 2005.
- [11] N. Yu, J. Fan, Q. Wang, C. Pflügl, L. Diehl, T. Edamura, M. i. Yamanishi, H. Kan, and F. Capasso, "Small-divergence semiconductor lasers by plasmonic collimation," *Nat. Photon.*, vol. 2, no. 9, pp. 564–570, Sep. 2008.
- [12] N. Yu, R. Blanchard, J. Fan, Q. Wang, C. Pflügl, L. Diehl, T. Edamura, M. Yamanishi, H. Kan, and F. Capasso, "Quantum cascade lasers with integrated plasmonic antenna-array collimators," *Opt. Express*, vol. 16, no. 24, pp. 19 447–19 461, Nov. 2008.
- [13] N. Yu, R. Blanchard, J. Fan, F. Capasso, C. Pflügl, L. Diehl, T. Edamura, M. Yamanishi, and H. Kan, "Small divergence edge-emitting semiconductor lasers with two-dimensional plasmonic collimators," *Appl. Phys. Lett.*, vol. 93, no. 18, p. 181101, Nov. 2008.
- [14] Z. B. Li, J. G. Tian, Z. B. Liu, W. Y. Zhou, and C. P. Zhang, "Enhanced light transmission through a single subwavelength aperture in layered films consisting of metal and dielectric," *Opt. Express*, vol. 13, no. 22, pp. 9071–9077, 2005.
- [15] D. Z. Lin, C. K. Chang, Y. C. Chen, D. L. Yang, M. W. Lin, J. T. Yeh, J. M. Liu, C. H. Kuan, C. S. Yeh, and C. K. Lee, "Beaming light from a subwavelength metal slit surrounded by dielectric surface gratings," *Opt. Express*, vol. 14, no. 8, pp. 3503–3511, Apr. 2006.
- [16] T. W. Ebbesen, H. J. Lezec, H. F. Ghaemi, T. Thio, and P. A. Wolff, "Extraordinary optical transmission through sub-wavelength hole arrays," *Nature*, vol. 391, no. 6668, pp. 667–669, Feb. 1998.
- [17] C. Genet and T. W. Ebbesen, "Light in tiny holes," *Nature*, vol. 445, no. 7123, pp. 39–46, Jan. 2007.
- [18] Y. Xie, A. Zakharian, J. Moloney, and M. Mansuripur, "Transmission of light through slit apertures in metallic films," *Opt. Express*, vol. 12, no. 25, pp. 6106–6121, Dec. 2004.
- [19] Y. Cui and X. He, "Enhancing extraordinary transmission of light through a metallic nanoslit with a nanocavity antenna," *Opt. Lett.*, vol. 34, no. 1, pp. 16–18, Jan. 2009.
- [20] Y. Wang, X. Zhang, H. Tang, K. Yang, Y. Wang, Y. Song, T. Wei, and C. H. Wang, "A tunable unidirectional surface plasmon polaritons source," *Opt. Express*, vol. 17, no. 22, pp. 20 457–20 464, Oct. 2009.

- [21] P. B. Johnson and R. W. Christie, "Optical constants of the noble metals," *Phys. Rev. B, Condens. Matter*, vol. 6, no. 12, pp. 4370–4379, Dec. 1972.
- [22] P. Lalanne, J. P. Hugonin, and J. C. Rodier, "Theory of surface plasmon generation at nanoslit apertures," *Phys. Rev. Lett.*, vol. 95, no. 26, p. 263902, Dec. 2005.
- [23] Z. Sun and H. K. Kim, "Refractive transmission of light and beam shaping with metallic nano-optic lenses," *Appl. Phys. Lett.*, vol. 85, no. 4, pp. 642–644, Jul. 2004.
- [24] Z. Li, Y. Yang, X. Kong, W. Zhou, and J. Tian, "Fabry–Perot resonance in slit and grooves to enhance the transmission through a single subwavelength slit," *J. Opt. A*, vol. 11, no. 10, p. 105002, Aug. 2009.
- [25] F. Lopez-Tejiera, S. G. Rodrigo, and L. Martin-Moreno, "Efficient unidirectional nanoslit couplers for surface plasmons," *Nat. Phys.*, vol. 3, pp. 324–328, May 2007.
- [26] P. Lalanne and J. P. Hugonin, "Interaction between optical nano-objects at metallo-dielectric interfaces," *Nat. Phys.*, vol. 2, no. 8, pp. 551–556, Jul. 2006.